# Drug Binding by Branched DNA: Selective Interaction of Tetrapyridyl Porphyrins with an Immobile Junction†

Min Lu,‡ Qiu Guo,‡ Robert F. Pasternack,§ Donald J. Wink,‡ Nadrian C. Seeman,‡ and Neville R. Kallenbach*,‡

*Department of Chemistry, New York University, New York, New York 10003, and Department of Chemistry, Swarthmore College, Swarthmore, Pennsylvania 19081*

*Received July 11, 1989; Revised Manuscript Received September 21, 1989*

ABSTRACT: The differential binding of a number of water-soluble cationic porphyrins to a branched DNA molecule is reported. Tetrakis(4-*N*-methylpyridiniumyl)porphine ($H_2$TMpyP-4) interacts near the branch point with an immobile DNA junction formed from four 16-mer strands. Its Cu(II) and Ni(II) derivatives show stronger preferential binding in the neighborhood of the branch point. Axially liganded derivatives, Zn, Co, and Mn, also interact near this branch point, but in a different way. We use the reagents methidiumpropyl-EDTA·Fe(II) [MPE·Fe(II)] and bis(*o*-phenanthroline)copper(I) [$(OP)_2$Cu(I)] to cleave complexes of DNA duplex controls and the junction with these porphyrins. The resulting cleavage patterns are consistent with previous evidence that the branch point provides a strong site for intercalative binding agents, which is not available in unbranched duplexes of identical sequence. The preferential scission by $(OP)_2$Cu(I) in the presence of Ni and Cu porphyrins near the branch point exceeds that seen for any agents we have studied. This hyperreactivity is not seen in the case of porphyrins with axial ligands, ZnTMpyP-4, CoTMpyP-4, and MnTMpyP-4, although these also interact near the branch point. The Zn derivative tends to protect sites close to the branch point from cutting, while the Co and Mn porphyrins moderately enhance cleavage of sites in this region.

Certain planar polycyclic aromatic molecules can interact with DNA or RNA by means of intercalative binding modes, in which the ring system inserts between adjacent base pairs to form a sandwich with the plane of the ring(s) roughly parallel to that of the bases (Lerman, 1961). These include a number of drugs, such as ethidium, quinacrine, or daunomycin, mutagens such as the acridines, and antibiotics like actinomycins, as well as many carcinogens. The most direct evidence for intercalation comes from X-ray diffraction analysis of crystalline complexes of planar polycycles in oligonucleotides [e.g., Quigley et al. (1986)]. Unwinding of superhelical turns in closed covalent circles of duplex DNA (Wang, 1974) or an increase in the length and stiffness of DNA, monitored by viscosity or linear dichroism changes (Cohen & Eisenberg, 1969), are diagnostic criteria in solution (Bloomfield et al., 1974; Cantor & Schimmel, 1980). In addition, NMR provides important information: the chemical shifts of imino and aromatic protons of bases and of aromatic protons in ring systems which are deshielded by the respective ring currents move upfield on intercalation (Krugh & Reinhardt, 1975; Young & Kallenbach, 1981). Downfield shifts of $^{31}$P resonances of the phosphates flanking the site of intercalation of a ring system are also observed [see Gorenstein (1984)].

Some features that are less diagnostic are based on the enhanced thermal stability of DNA ($T_m$) resulting from intercalation (Crothers, 1971) or the longer lifetime of intercalated complexes (Pasternack et al., 1983a). These can also accompany other modes of tight binding. Particular spectral properties of the intercalated rings, such as induced CD signals in drug absorption bands (Gardner & Mason, 1967) or changes in absorption or emission frequencies or intensities of these bands, may also reflect interaction with the bases (Lepecq & Paoletti, 1967).

Among the most remarkable and perhaps unlikely systems that have been asserted to exhibit intercalative binding modes are a group of water-soluble cationic porphyrins (see Figure 1); porphyrins are large fused systems of heterocycles which play essential roles as prosthetic groups in many proteins and enzymes [see, e.g., Stryer (1988)]. While no X-ray crystal structures of intercalated porphyrin–DNA complexes have yet been reported, the water-soluble meso-substituted porphyrin tetrakis(4-*N*-methylpyridiniumyl)porphine ($H_2$TMpyP-4) was first proposed to exhibit intercalative modes of binding by Fiel and his co-workers (Fiel et al., 1979) on the basis of viscosity measurements, increase in $T_m$, and unwinding studies of circular DNA. The interaction of $H_2$TMpyP-4 with covalently closed DNA circles is accompanied by a degree of unwinding that is almost identical with that of ethidium (Kelly et al., 1985). Intercalative modes appear to be strongly favored only for alternating CpG sequences (Pasternack et al., 1983b; Marzilli et al., 1986). NMR measurements using $^1$H and $^{31}$P detect the presence of at least one type of complex in which the porphine ring appears to insert fully and symmetrically between adjacent CpG base pairs (Ford et al., 1987). However, only in a pure CG sequence could this represent the exclusive or dominant mode of binding. Intercalation has been shown to take place in mixed sequences containing some GC base pairs (Gibbs et al., 1988; Fiel, 1989). In addition, some mode or modes of external binding take place with A·T or mixed sequences (Carvlin et al., 1983; Pasternack et al., 1983b; Marzilli et al., 1986; Banville et al., 1986). Similar intercalative modes are observed for the tetrakis(3-*N*-methylpyridiniumyl)porphine, but the tetrakis(2-*N*-methylpyridiniumyl)porphine appears to be incapable of intercalation (Carvlin & Fiel, 1983; Pasternack et al., 1983b), presumably

† This work was supported by Grants CA-24101, GM-29554, and GM-34676 from the National Institutes of Health.

* Author to whom correspondence should be addressed.

‡ New York University.

§ Swarthmore College.

0006-2960/90/0429-1614$02.50/0 

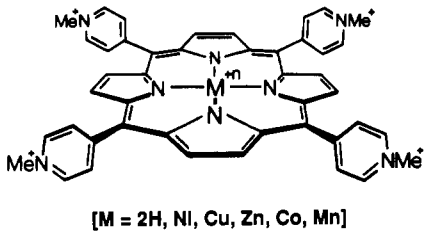


[M = 2H, Ni, Cu, Zn, Co, Mn]

FIGURE 1: Structural formulas of 5,10,15,20-tetrakis(*N*-methylpyridinium-4-yl)porphyrin and its complexes with hydrogen or metal ligands. The position of the methyl substituent on the pyridinium appears to have an important role in the interaction of these porphyrins with DNA (Fiel, 1989): the 3-*N*-methyl and the 4-*N*-methyl derivatives illustrated both permit intercalative binding, while the 2-*N*-methylpyridinium species can only bind externally. The metal ligand also exerts a strong effect on potential intercalative binding (Gibbs et al., 1988): axially unliganded metal derivatives may intercalate, while axially liganded species cannot.

because of steric hindrance by the meso ring systems.

The interaction of these molecules with DNA is modulated strongly by the presence and nature of metal ligands on the porphine [see Gibbs et al. (1988) or Fiel (1989) for recent reviews]. The basic observation is that metal derivatives lacking axial ligands, Cu(II) and Ni(II), for example, behave like $H_2$TMpyP-4 in exhibiting intercalative binding modes, with preference for CG sites (Pasternack et al., 1983b). Metal derivatives that possess axial ligands, such as Zn(II), Co(III), Fe(III), or Mn(III), appear to be incapable of traditional intercalation and interact instead via external modes (Pasternack et al., 1983b), with a preference for the minor groove of A·T sequences, as can be demonstrated most directly by porphyrin-mediated chemical cleavage of DNA (Ward et al., 1986; Bromley et al., 1986).

Here we examine the binding of $H_2$TMpyP-4, two axially unliganded metal complexes, CuTMpyP-4 and NiTMpyP-4, and three axially liganded porphyrins, ZnTMpyP-4, CoTMpyP-4, and MnTMpyP-4, to a branched DNA molecule. It has been reported that branched DNA interacts with intercalative drugs differently from linear duplexes (Guo et al., 1989, 1990). Methidium and propidium bind preferentially at a site near the branch point in an immobile four-arm branched structure (Seeman, 1982; Seeman & Kallenbach, 1983) formed from four 16-mers, which we refer to as J1 (Figure 2). Many features of J1 have been characterized (Kallenbach et al., 1983; Wemmer et al., 1985; Seeman, et al., 1985; Marky et al., 1987; Petrillo et al., 1988). The geometry shown in Figure 2 suggests an overall 2-fold symmetry of the two helical stacks, consistent with Fe(II)·EDTA cutting experiments (Churchill et al., 1988) as well as with electrophoretic studies (Cooper & Hagerman, 1987; Duckett et al., 1988; Seeman et al., 1989).

Footprinting analysis (Galas & Schmitz, 1978; Schmitz & Galas, 1979) of propidium binding to J1 using the nucleolytic activity of methidiumpropyl-EDTA iron [MPE·Fe(II)] and bis(*o*-phenanthroline)copper(I) [$(OP)_2$Cu(I)] reveals the pattern of enhancement of scission indicated in Figure 2, relative to linear duplexes with the same sequence (Guo et al., 1989, 1990). This pattern is roughly 2-fold symmetric, centered near the branch point of the model of J1 (Figure 2). The bulkier actinomycin D molecule does not compete with propidium for this site (Guo et al., 1990).

Our current picture of drug binding by J1 is that the branch point has two phosphates nearly apposed at the crossover point, which favors cation binding (Guo et al., 1989). In addition, there is possibly also a structural perturbation that facilitates intercalation. It is then of interest to explore the response of

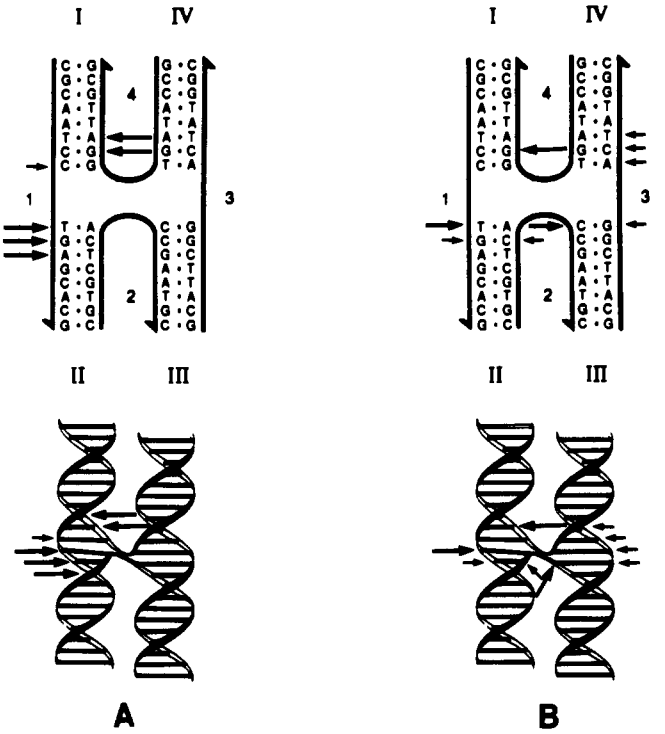


FIGURE 2: Sequence and structure of the branched junction J1 and its cleavage by MPE·Fe(II) and $(OP)_2$Cu(I). The upper panels show the junction in schematic, while the lower panels show a model of the junctions based on 10.5-fold B-DNA. The junction consists of four strands of DNA, indicated in the upper panel by Arabic numerals. Each strand participates in forming two double-helical arms, indicated by Roman numerals. Note that the branch point occurs between positions 8 and 9 on each strand. The structural conclusion of previous work (Churchill et al., 1988) is indicated in this figure by stacking arm I on arm II and arm III on arm IV to form two helical domains. The results of the scission experiments previously reported (Guo et al., 1989, 1990) are summarized in this figure, using the antiparallel conformer of J1 which we believe to be the predominant form in solution (Seeman et al., 1989). Sites of differential cleavage due to the interaction of J1 with MPE·Fe(II) are indicated by arrows in panel A. The length of the arrow is a measure of the quantitative intensity of each responsive site. Panel B shows those sites due to the interaction of J1 with $(OP)_2$Cu(I).

this site, which in principle is larger than any corresponding site in a linear duplex, to binding by extended ring systems, including the porphyrins. We show here that $H_2$TMpyP-4 and its axially unliganded complexes with Cu(II) and Ni(II) interact preferentially at the crossover site, with the latter two inducing a much stronger response to $(OP)_2$Cu(I) cleavage than does propidium. The axially liganded Zn(II), Co(III), and Mn(III) complexes also respond in the vicinity of this site, but with quite different characteristics which we suggest may be associated with partial intercalative modes of interaction.

## Materials and Methods

*Porphyrins.* The free base porphyrins $H_2$TMpyP-2 and $H_2$TMpyP-4 were purchased as the tetrachlorides from Mid-Century Chemical Co. Metal derivatives of the latter species are prepared following published procedures in each case (Pasternack et al., 1973, 1974; Pasternack & Cobb, 1973; Harriman & Porter, 1979). Concentrations of porphyrins are determined spectrophotometrically with a modified Cary 118 instrument. Molar absorptivities that are used are summarized in Table I.

*Nucleic Acids.* All DNA strands used in these experiments are synthesized on an ABI 380B automated synthesizer, using standard phosphoramidite chemistry (Caruthers, 1982). Strands are purified following deprotection and removal from

Table I: Extinction Coefficients of the Porphyrins Used in This Study

| compound | solvent | λ (nm) | ε ($M^{-1}$ $cm^{-1}$) | reference |
|---|---|---|---|---|
| $H_2$TMpyP-2 | $H_2O$ | 414 | $1.82 \times 10^5$ | Pasternack et al., 1973 |
| $H_2$TMpyP-4 | $H_2O$ | 423 | $2.26 \times 10^5$ | Hambright et al., 1976 |
| CuTMpyP-4 | $H_2O$ | 424 | $2.31 \times 10^5$ | Pasternack et al., 1973 |
| NiTMpyP-4 | $H_2O$, 20% acetone | 418 | $1.49 \times 10^5$ | Pasternack et al., 1974 |
| CoTMpyP-4 | 0.01 M $HNO_3$ | 434 | $2.15 \times 10^5$ | Pasternack & Cobb, 1973 |
| ZnTMpyP-4 | $H_2O$ | 434 | $2.04 \times 10^5$ | Pasternack et al., 1973 |
| MnTMpyP-4 | $H_2O$ | 463 | $9.20 \times 10^4$ | Harriman & Porter, 1979 |

the synthetic columns by preparative HPLC on a Du Pont Zorbax Bio Series oligonucleotide column, using a NaCl gradient in a solvent system containing 20% acetonitrile and 80% 0.02 M sodium phosphate. Fractions from the major peak are collected, concentrated, desalted, and lyophilized.

*Phosphorylation and Strand Purification.* Twenty micrograms of a specific DNA strand is dissolved in 10 μL of a solution containing 66 mM Tris·HCl, 1 mM spermidine, 10 mM $MgCl_2$, 15 mM dithiothreitol (DTT), and 0.2 mg/mL nuclease-free bovine serum albumin (BSA) from BRL and mixed with 5 μL of 1.25 mM [γ-$^{32}$P]ATP (10 mCi/mL) and 2 units of T4 polynucleotide kinase (Boehringer) for 15 min at 37 °C. This reaction is quenched by adding 1 mM of cold ATP and 1 unit of T4 polynucleotide kinase and stopped by freezing in dry ice. The mixture is rapidly heated for 5 min at 70 °C, cooled to room temperature, and loaded on a 20% denaturing polyacrylamide gel. The gel is run at 2000 V (ca. 50 V/cm) for 3 h at room temperature and exposed briefly to X-ray film (Kodak X-Omat AR or Amersham Hyperfilm βmax); the band corresponding to 16-mer is cut out and soaked overnight at 37 °C in 0.5 mL of buffer (0.5 M ammonium acetate, 1 mM EDTA). This material is centrifuged for 5 min at room temperature in a microfuge, and the gel is reextracted with 0.1 mL of the same buffer, precipitated twice with ethanol, and lyophilized.

*MPE·Fe(II) Cutting.* Our procedure follows that of Van Dyke and Dervan (1983a,b), with minor changes due to the short strands involved and the addition of $Mg^{2+}$ to stabilize junctions (Seeman et al., 1985). Junctions are formed by annealing a stoichiometric mix of strands at 16 μM concentration in 50 mM Tris·HCl, pH 7.5, with 10 mM $MgCl_2$. An Eppendorf tube containing the solution is immersed in boiling water for 2 min, cooled slowly to room temperature, and finally chilled to 4 °C. Double-stranded controls are formed similarly, by using a stoichiometric amount of cold strand complementary to the labeled junction strand. For cutting both branched and linear molecules, freshly prepared solutions of MPE·Fe(II) are made up in a buffer of 10 mM Tris·HCl, pH 7.4, with 50 mM NaCl, containing 1 μM Fe(II) and 2 μM MPE (Van Dyke & Dervan, 1983a,b). DNA (16 μM) is exposed to the reagent for 15 min at 4 °C, followed by addition of 4 mM DTT for 30 min, and the reaction is stopped by freezing on dry ice. After extraction with 1-butanol to remove drug and drying, the sample is taken up in formamide loading buffer, heated briefly to 90 °C, cooled, and then run on a denaturing polyacrylamide gel for 3 h at 2000 V (ca. 50 V/cm) and 40 °C. No dyes are added in these runs. The gel is dried immediately on a vacuum drying apparatus (Hoefer) and exposed at room temperature to film without an intensifier screen.

*$(OP)_2$Cu(I) Cutting.* For cutting branched and linear molecules, freshly prepared solutions of 200 mM *o*-phenanthroline (Kodak), 45 mM $CuSO_4$, and 1 mM ascorbate (replacing 3-mercaptopropionic acid; Kuwabara et al., 1986) are made up in a buffer of 50 mM Tris·HCl, pH 7.5, with 10 mM $MgCl_2$. The DNA is exposed to the reagent for 45 min at 4 °C, followed by extraction with 1-butanol and drying. The sample is taken up in formamide loading buffer, heated briefly to 90 °C, cooled, and run on a denaturing polyacrylamide gel for 3 h at 2000 V (ca 50 V/cm) and 40 °C. No dyes are added in these runs. The gel is dried immediately on a vacuum drying apparatus (Hoefer) and exposed at room temperature to X-ray film without an intensifier screen.

*Densitometry and Comparison of Profiles.* Autoradiograms are scanned on a Hoefer GS300 densitometer or an LKB Ultroscan XL laser densitometer. No base-line corrections are applied. The data from the experiments we report consist of pairs of profiles corresponding to the relative probability of chain scission at a series of positions with respect to a labeled 5′-phosphate for each strand in a DNA 16-mer duplex and in the junction tetramer. These profiles can differ in the *overall* intensity of scission, as well as the *relative* intensity at individual bands. In many cases, it is possible to select a set of three or more bands with comparable relative intensities and use these to normalize two profiles by eye. These bands often lie near the chain termini, where effects from the branch site might be expected to be less evident. We identify positions of enhancement or protection relative to these benchmarks. However, in some cases, differences seen in the presence of porphyrin are so drastic that no such benchmarks can be identified. Our procedure is to cite only positions that we see as different in relative intensity and that are outside the correction one could apply by normalizing. Thus we have avoided pointing out a number of "differences" in the profiles presented in Figures 3–7, although some might nevertheless be real. From repeated scans of autoradiograms, intensity differences of ±10% are probably not significant.

## Results

Our procedure is to measure the probability of a chain scission by $(OP)_2$Cu(I) or MPE·Fe(II) using a particular 5′-$^{32}$P-labeled strand, say strand 1, in parallel experiments: (i) paired with its 16-mer complement to form an uninterrupted double-stranded duplex and (ii) paired with strands 2–4 in the tetrameric junction (Churchill et al., 1988; Chen et al., 1988; Guo et al., 1989, 1990). Doing this for each of the four strands of the tetramer reveals sites of potential differences between each duplex and the tetramer, due presumably to structural effects present in the latter. We have reported that both MPE·Fe(II) and $(OP)_2$Cu(I) show a pattern of enhanced probabilities of cleavage at positions near the branch point in J1 (Guo et al., 1989, 1990). Here, we investigate first the binding properties of three presumptive porphyrin intercalators, $H_2$TMpyP-4, and its Cu (II) and Ni (II) derivatives (Gibbs et al., 1988), using these reagents. We then describe the behavior of three nonintercalative species, the Zn, Co, and Mn derivatives.

In analyzing the data, two kinds of comparison are made: (i) duplex + porphyrin vs free duplex, monitoring any *sequence preferences* in linear DNA; and (ii) junction + porphyrin vs duplex + porphyrin, looking for *differential* effects in the branched molecule absent in linear duplexes. The latter differential effects are contrasted with the reference differential


FIGURE 3: Densitometric scans of the cleavage pattern of J1 due to MPE·Fe(II) and MPE·Fe(II) competing with $H_2$TMpyP-4 and its Ni(II) and Cu(II) derivatives. Each column of this figure corresponds to a given strand of J1 and contains four panels. Panel A shows densitometric scans of the cleavage pattern of J1 by MPE·Fe(II); panel B shows densitometric scans of the cleavage pattern of J1 due to MPE·Fe(II) competing with $H_2$TMpyP-4; panel C is due to MPE·Fe(II) competing with NiTMpyP-4; and panel D is due to MPE·Fe(II) competing with CuTMpyP-4. Each panel of scans contains two scans, one with the strand labeled in the tetrametric junction (J) and one with the strand labeled in linear duplex formed with its complementary strand (ds). Sites of differential enhancement in this experiment are indicated as black bands in ds and J. Sites of differential protection are indicated by filled circles over the corresponding bands in the J profiles. These profiles and those in Figures 4–6 are discussed in detail in the text.

pattern shown by the junction and duplex in the absence of porphyrin to assess the net effect of porphyrin on the junction.

For reference, the top panels in Figures 3–6 compare the relative probabilities of chain scission at different positions in each strand of the junction, J1, with those of scission at the corresponding positions in the four 16-mer duplexes, all in the *absence* of porphyrins. Figures 3A and 5A show the results when MPE·Fe(II) is used as a probe, and Figures 4A and 6A show the effect of cleavage by $(OP)_2$Cu(I) (Guo et al., 1990). Each probe reacts distinctively with the branched structure relative to the corresponding duplexes: MPE·Fe(II) cuts preferentially at positions **1**:9–11 and **4**:10,11 (Figure 3A) while $(OP)_2$Cu(I) shows enhanced cutting at positions **1**:9,10, **2**:7,9, and **3**:8–11 as well as at **4**:10[1] (Figure 4A). In addition, as we have noted (Guo et al., 1989), positions flanking sites of enhancement show a pattern of protection: if we accept the bands **1**:8 and 12 as standards (see Materials and Methods), positions **1**:6,7,13–15 are protected in the junction (Figure 3A, ds vs J). Picking **4**:9 and **4**:12 as standards, positions **4**:5–8,13–15 are also protected. Since there is no corresponding effect in scission induced by the nonintercalator $(OP)_2$Cu(I), the protection might represent neighbor site exclusion (Berman

[1] Our notation indicates the number of the strand, say **i** (Figure 2), in boldface and the site of origin of the cut by a number following a colon, **i**:*j*. The major fragment resulting fram radical scission of the phosphodiester at position *j* is the 3′-phosphomonoester with *j* − 1 nucleosides and 5′- and 3′-terminal phosphates (Kuwabara et al., 1986).

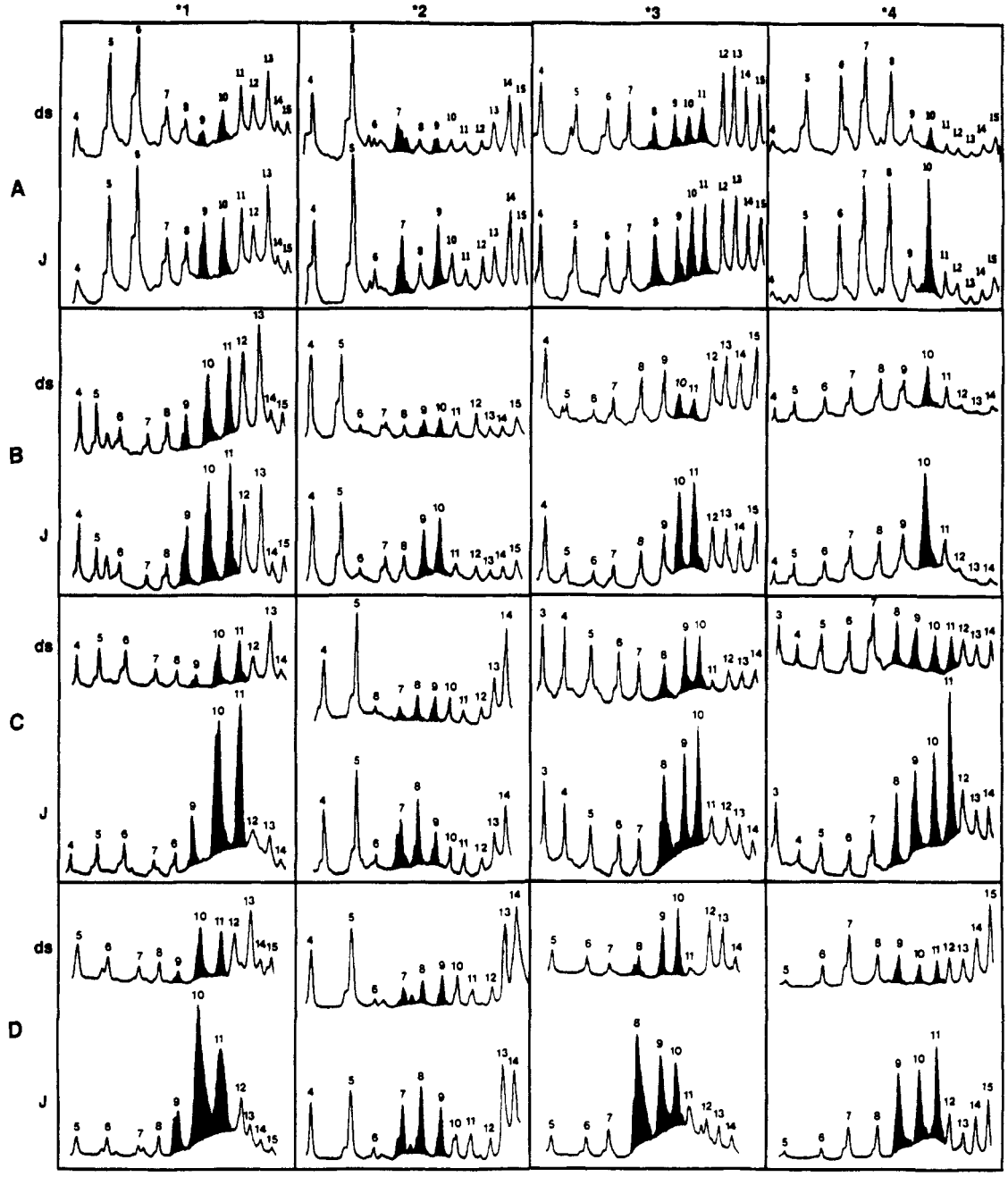


FIGURE 4: Densitometric scans of the cleavage pattern of J1 due to $(OP)_2Cu(I)$ and $(OP)_2Cu(I)$ competing with $H_2TMpyP$-4 and its Ni(II) and Cu(II) derivatives. The same conventions apply to this figure as to Figure 3.

& Young, 1981) in the case of the 6–8 bands and possibly occlusion from the opposite duplex in the junction for the 13–15 bands, which can interact if the two duplexes in Figure 2 lie essentially parallel to each other as drawn.

The effect of the four porphyrins studied on the scission patterns of duplexes and tetramer is presented in Figures 3–6, panels B–D.

*$H_2TMpyP$-4.* Figure 3B shows the pattern of MPE·Fe(II)-induced scission resulting when $H_2TMpyP$-4 is added to the duplex and tetramer DNAs at a molar ratio of 2:1. In the presence of porphyrin, the probability of cutting of each duplex is distinctly altered (Figure 3A-ds vs Figure 3B-ds), indicating binding of the porphyrin: positions **1**:6(T),7(C),13–14(CA), **2**:9(C),14(T),15(G), **3**:12–14(ATG), and **4**:13,14(TG) show clear protection in the presence of $H_2TMpyP$-4, with no pronounced sequence preference as shown by the identities of the bases in parentheses. On the other hand, the *differential* MPE·Fe(II) profiles of the strands in the tetramer with respect to the duplexes (compare Figure 3B-J with Figure 3A-J) are very similar to those of the tetramer in the absence of porphyrin, showing enhanced scission near the branch point at positions **1**:9–11 and **4**:10,11. Strand **2** however, shows a hint of protection in the tetramer at position 9, adjacent to the branch point. Thus MPE·Fe(II) provides only marginal evidence for preferential interaction of $H_2TMpyP$-4 with J1. This may be due to the inability of $H_2TMpy$-4 at the concentration used to compete with MPE·Fe(II) for the branch point.

The effects in the profiles derived from $(OP)_2Cu(I)$ are more evident (Figure 4B), but the differential effect between duplexes and tetramer is similar to that revealed by MPE·Fe(II). The *duplex* patterns (Figure 4A-ds and 4B-ds) drastically change with addition of porphyrin, for example, at **1**:5,6,12, **2**:14,15, **3**:5,6,8–11, and **4**:5–8. Enhancement in reactivity at **1**:9–11, **2**:9,10, **3**:10,11, and **4**:10 is apparent in the *tetramer* (Figure 4B-J) with respect to the *dimer* (Figure 4B-ds), mostly


FIGURE 5: Densitometric scans of the cleavage pattern of J1 due to MPE·Fe(II) and MPE·Fe(II) competing with Zn, Co, and Mn derivatives of $H_2$TMpyP-4. The same conventions apply to this figure as to Figure 3. Panel A shows densitometric scans of the cleavage pattern of J1 by MPE·Fe(II); panel B shows densitometric scans of the cleavage pattern of J1 due to MPE·Fe(II) competing with ZnTMpyP-4; panel C is due to MPE-Fe(II) competing with CoTMpyP-4; and panel D is due to MPE·Fe(II) competing with MnTMpyP-4.

at sites that show enhancement in the absence of porphyrin. The major difference associated with presence of the porphyrin occurs at **2**:10.

Since $(OP)_2Cu(I)$ appears to detect scission over its actual site of interaction (Kuwabara et al., 1986), $H_2$TMpyP-4 does in fact appear to bind the junction in the vicinity of the branch point, as can be detected by the effects in strand **2** alone by using both probes.

*NiTMpyP-4 and CuTMpyP-4.* A stronger differential signal is seen for the Ni and Cu derivatives of $H_2$TMpyP-4, as shown in panels C and D of Figures 3 and 4. Again, the MPE·Fe(II) cutting patterns of the duplexes are changed by the presence of porphyrin (compare the ds panel in 3A). Comparing junction with duplexes, the MPE·Fe(II) experiments in Figure 3C,D show that the enhancement observed at **1**:9–11 and **4**:10,11 (Figure 3A) in the free junction with respect to free duplexes is *diminished* to become a relative protection, by both these porphyrins, more fully in the case of Ni than Cu. This is consistent with inhibition or partial inhibition of the strong methidium site in J1 for MPE·Fe(II) by these porphyrins, and this effect has been noted also when propidium is used to compete with MPE in J1 (Guo et al., 1989).

Interestingly, the protection of sites in the junction at **1**:6,7 (Figure 3A-J vs 3A-ds) which is near the site of enhanced cutting in strand **1** does not persist in the presence of the $H_2$ and Cu porphyrins. The site in strand **4**, at **4**:5–8, shrinks to only **4**:7 or **4**:8, respectively, depending on the porphyrin. This is not inconsistent with the idea that the protection is due to exclusion of these positions to MPE by a next-neighbor effect exerted from the adjacent tight binding site.

The results for CuTMpyP-4 and NiTMpyP-4 probed by $(OP)_2Cu(I)$ are more striking (Figure 4B,C). These two porphyrins cause a significant perturbation of the patterns of duplexes alone. Comparison of junction vs duplex cutting now shows quantitatively different effects at positions **1**:9–11, **2**:7–9,

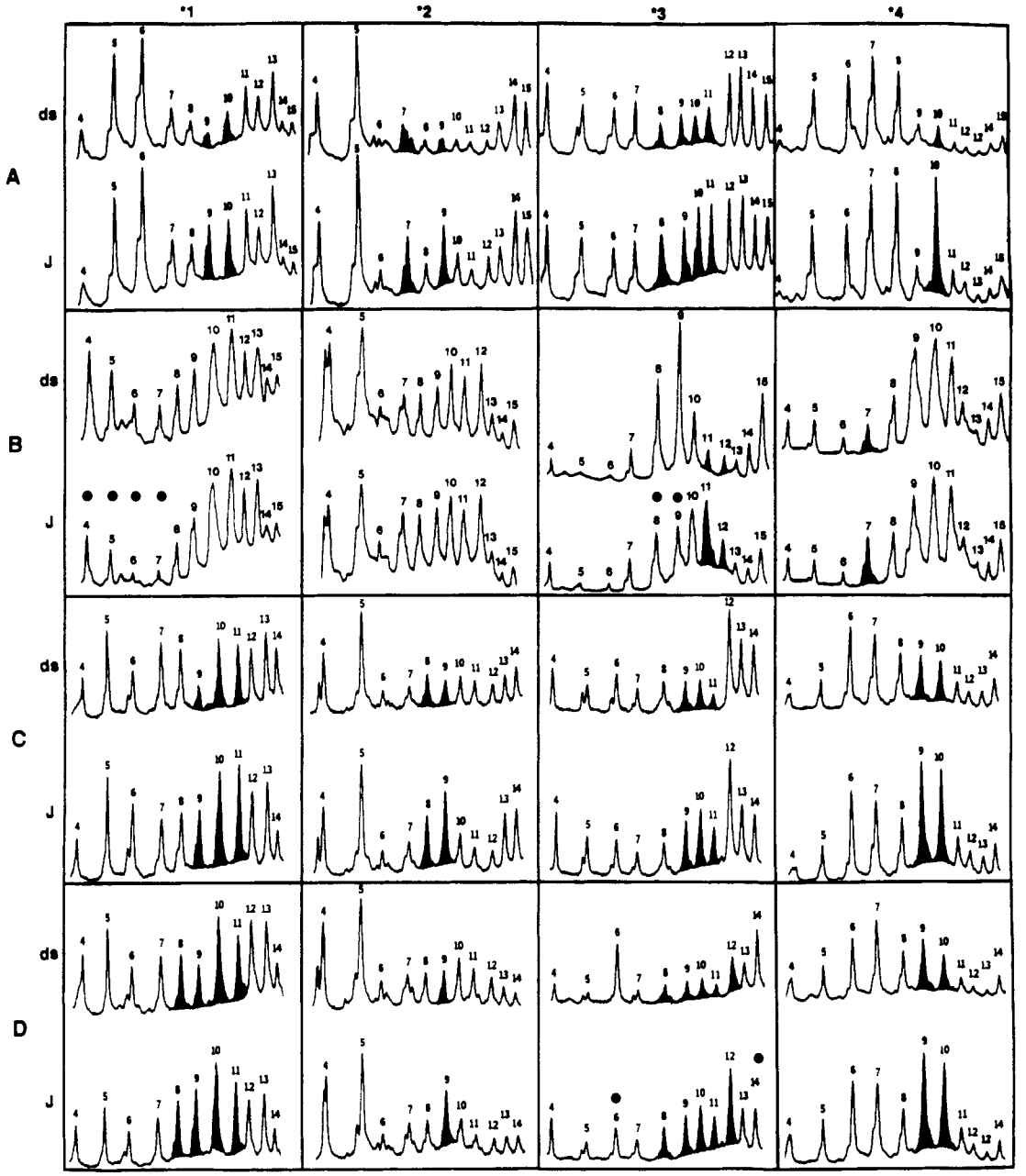


FIGURE 6: Densitometric scans of the cleavage pattern of J1 due to $(OP)_2Cu(I)$ and $(OP)_2Cu(I)$ competing with Zn, Co, and Mn derivatives of $H_2TMpyP$-4. The same conventions apply to this figure as to Figures 3 and 5.

3:8–10, and 4:8–11, distinct in most cases from the corresponding effects in the absence of porphyrin (Figure 4A). Positions 1:10 and 11, for example, become hyperreactive in the presence of either Cu- or NiTMpyP-4, in contrast to the moderate enhancement seen at these positions in the free junction or with $H_2TMpyP$-4. Position 2:8 becomes more reactive than 2:7 and 2:9 in the presence of these porphyrins, while it is less so in the free junction or with $H_2TMpyP$-4. Positions 4:9 and 11 also become strongly reactive in the presence of the metalloporphyrins, and marginally so in the absence of these agents. The positions of enhanced reactivity for $(OP)_2Cu(I)$ lie around the branch point per se, with a rough 2-fold symmetry, although distinct patterns are seen on each arm in detail.

Since each of the above porphyrins has been asserted to be capable of intercalation into duplex DNA (Pasternack et al., 1983b; Gibbs et al., 1988; Fiel, 1989), it is tempting to attribute the behavior of these three porphyrins to an intercalative interaction at or very near the branch point in J1. However, it would be premature to attempt to reach structural conclusions from footprinting data of any kind. One way to test this hypothesis is to compare the above results with the Zn, Co, and Mn derivatives of TMpyP-4, which contain one or more axial ligands and which are not thought to be capable of intercalation into duplex DNA (Pasternack et al., 1983b), possibly because of simple steric hindrance by the axial ligands. Figures 5 and 6 compare the cutting profiles of complexes of these porphyrins with duplex DNAs and with the junction.

*ZnTMpyP-4, CoTMpyP-4, and MnTMpyP-4.* The Zn derivative produces a completely different pattern of scission of each linear duplex with both MPE·Fe(II) (Figure 5B) and $(OP)_2Cu(I)$ (Figure 6B). Thus positions 1:6(T),7(C), 2:9-(C),14(T),15(G), 3:5(T),6(C),12–14(ATG), and 4:6(A),7-(G),13(T) are protected from MPE·Fe(II)-induced cleavage in the duplexes by ZnTMpyP-4 (parts A-ds and B-ds of Figure 5), while many more positions show protection or enhancement with respect to $(OP)_2Cu(I)$ cleavage in the absence of the porphyrin(parts A-ds and B-ds of Figure 6).

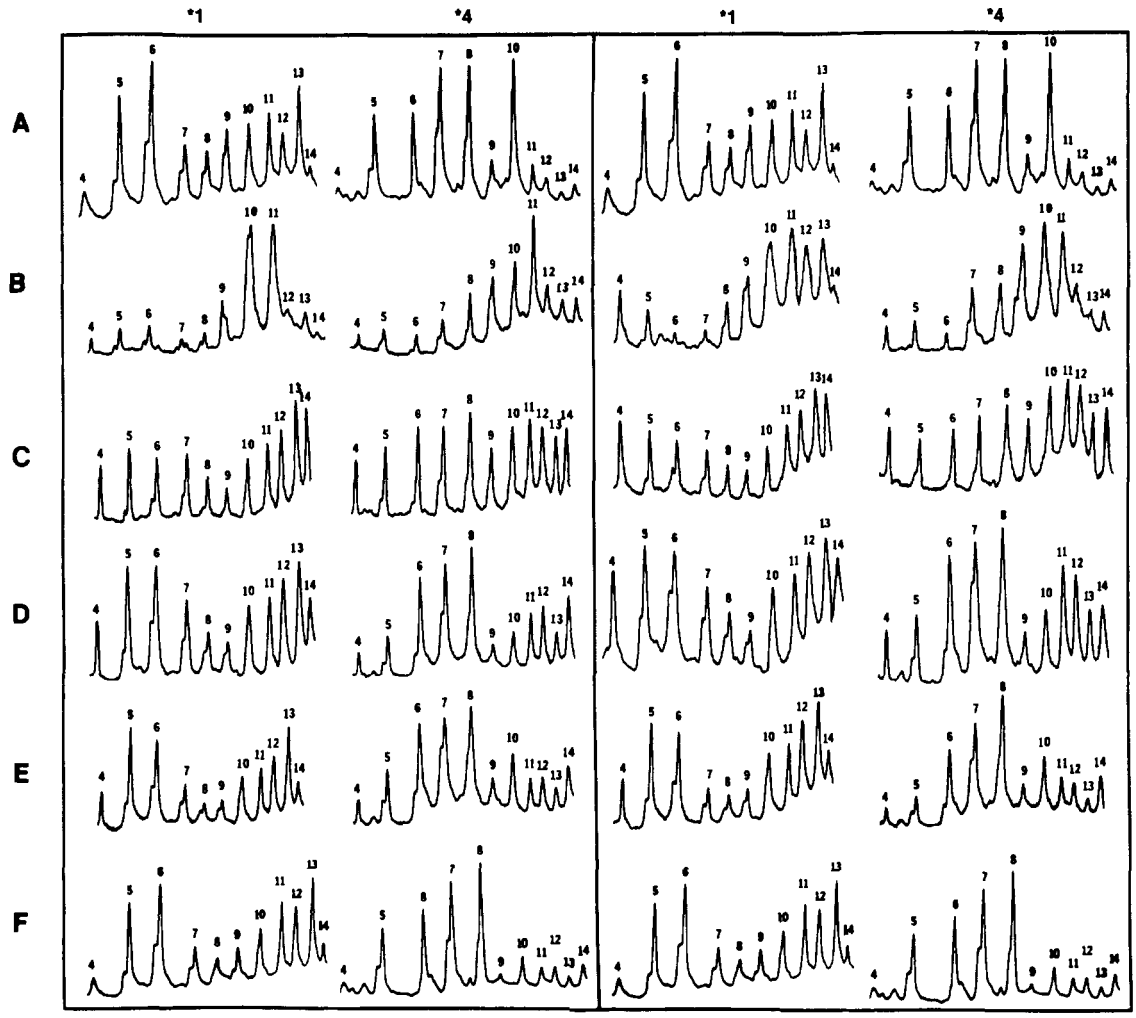


FIGURE 7: Densitometric scans of the cleavage pattern of J1 due to footprint of PI competing with Ni and Zn derivatives of $H_2$TMpyP-4 for binding to J1 cutting by $(OP)_2Cu(I)$. The left panel is the cleavage pattern of J1 due to footprint of PI competing with NiTMpyP-4, while the right panel is PI competing with ZnTMpyP-4. Each column of this figure corresponds to a given strand of J1. Each column of scans contains six scans: panel A is the $(OP)_2Cu(I)$ cleavage; panel B is 2:1 metal derivatives of $H_2$TMpyP-4 to J1 cutting by $(OP)_2Cu(I)$; panels C, D, and E are $^1/_2$-, 2-, and 8-fold propidium to J1 in the presence of 2:1 metal derivatives of $H_2$TMpyP-4 to J1 cutting by $(OP)_2Cu(I)$; and panel F is 2:1 propidium to J1 cutting by $(OP)_2Cu(I)$.

While positions affected in the duplexes tend to remain so in the tetramer profiles, there is evidence for a specific effect of ZnTMpyP-4 in the vicinity of the branch point. Comparing junction with duplex patterns in panels A and B of Figure 5 now, residues **1**:9–11 and **4**:10,11 are slightly less reactive (Figure 5B-J vs 5B-ds) in the junction than in the corresponding duplex with respect to MPE·Fe(II) scission (Figure 5A-J vs 5A-ds). Similarly, from panels A and B of Figure 6, we see that the characteristic enhancements in $(OP)_2Cu(I)$ cutting seen at **1**:9,10, **2**:7,9, **3**:8–11, and **4**:10 in the free junction are eliminated, **3**:9 again being protected. This is a specific interaction seemingly distinct from the previous three examples. Intercalation of the axially liganded ZnTMpyP-4 into J1 might be possible in principle, provided the site is sufficiently "open". However, the data suggest the binding mode is not similar to those involved in what we have proposed to be intercalative binding at the branch. Strong protection from $(OP)_2Cu(I)$-induced scission has been found in the case of netropsin, a drug that occupies the minor groove of adjacent AT sequences in double-stranded DNA (Kuwabara et al., 1987). By analogy, the ZnTMpyP-4 might lie in the minor groove(s) at the branch point without inserting completely. In this case, the porphyrin appears to inhibit cleavage relative to duplex, rather than enhancing it, particularly at **1**:6,7, as well as at **3**:9, as noted. However, a major enhancement is seen at **3**:11. It is possible to construct models of the junction (Seeman, 1988) with **3**:11 in proximity to **1**:6,7.

The Co and Mn derivatives of $H_2$TMpyP-4 (Figures 5C-ds and 6C-ds) also alter the pattern of the duplexes with respect to the controls in Figures 5A-ds and 6A-ds. Comparing the cutting of the junction vs duplexes, enhanced scission with MPE·Fe(II) is seen in the Co–J1 complex at **1**:9, **3**:6,10, and **4**:10,11 with inhibition at **1**:7, **2**:8–10, and **4**:8,9 compared to the duplex patterns in Figure 5C. But the enhancements in the free junction at **1**:10,11 and **4**:11 (Figure 5A) are either quantitatively lower than or absent in the presence of the CoTMpyP-4 molecule. Scission by $(OP)_2Cu(I)$ on the other hand produces enhanced reactivity in Co–J1 relative to duplexes with porphyrin at **1**:9–11, **2**:8,9, **3**:9–11, and **4**:9,10 (Figure 6C). These differ near the branch point from the differential pattern in free J1 relative to free duplexes (Figure 6A-j vs 6A-ds): **2**:7 (Figure 6C-ds vs 6C-J) is not enhanced as much in the Co–J1 complex, while **4**:9 is enhanced much more in the Co–J1 complex than in free J1.

The Mn derivative shows enhanced MPE·Fe(II) scission (Figure 5D-ds vs 5D-J) at **1**:8–11 and **3**:6,10,11, and protection at **4**:7–9; $(OP)_2Cu(I)$ shows enhanced reactivity at **1**:8–11, **2**:9, **3**:8–12, and **4**:9,10 (Figure 6d-ds vs 6D-J). These patterns resemble those of J1 with respect to free duplexes (Figures 5A-ds vs 5A-J and 6A-ds vs 6A-J). However, **3**:6 is protected

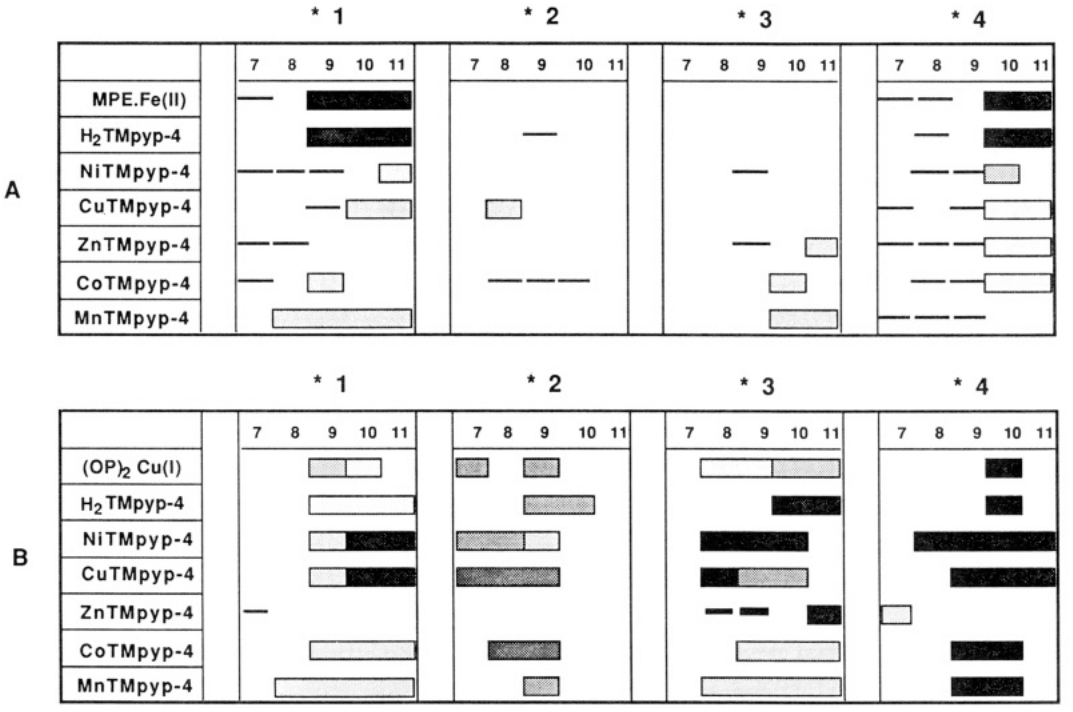


FIGURE 8: Summary of the differences in cleavage of the junction relative to duplexes observed in these experiments, in the absence and presence of the porphyrin derivatives indicated at the left. (A) Patterns from MPE·Fe(II)-induced cleavage in each of the strands numbered below as in Figure 2B. The corresponding patterns from $(OP)_2Cu(I)$-induced cleavage. Rectangles indicate positions that show enhanced reactivity of the probe, the darkness being roughly proportional to the intensity of enhancement observed. Solid horizontal lines indicate positions that show protection from scission by the probe, the thickness of the line being roughly proportional to the strength of protection.

in the Mn–J1 panel relative to the Mn–duplex (Figure 6D-ds vs 6D-J), and not in free J1 relative to free duplex. Again, **4**:9 is enhanced in Mn–J1 (Figure 6D-ds vs 6D-J), not in free J1.

Each of these metalloporphyrins thus shows some evidence for interaction near the branch point of the junction, as summarized in Figure 8. The interaction differs qualitatively and quantitatively from that seen in the case of the axially unliganded $H_2$, Ni, or Cu species. Returning to the question of whether the latter porphyrins actually interact with the junction via intercalation, we can perform a competition experiment similar to that carried out on MPE alone (Guo et al., 1989): propidium diiodide (PI) is an intercalative drug frequently used in DNA binding studies. It has the ethidium ring system, with a side chain having two positive charges.

Figure 7 shows the results of an experiment in which PI is used to compete for NiTMpyP-4 and ZnTMpyP-4 in binding J1. We monitor the response of the complexes to $(OP)_2Cu(I)$ cutting, since this is more sensitive than MPE·Fe(II), and we focus on the responsive bands at **1**:10,11 and **4**:9–11. Panel A shows the reference profile of these strands in free J1, probed by $(OP)_2Cu(I)$. Panel F shows the profile of the same strands in the presence of two moles PI per junction tetramer. This concentration of PI eliminates the strong enhancement in free J1 at **4**:10 and protects positions **1**:7–10 relative to free J1 (Guo et al., 1990). For reference, panel B shows the effect on the $(OP)_2Cu(I)$ cutting profile of J1 caused by the presence of 2 mol NiTMpyP-4 (on the left) and ZnTMpyP-4 (on the right). Addition of 0.5 mol of PI to the complex in panel B produces an intermediate pattern, panel C, which shows drastic reduction of the bands at **1**:10,11 and at **4**:11 in the Ni case. The Zn derivative does not show parallel reduction: positions **4**:9,11 remain enhanced in the Zn case up to equimolar addition of PI, in panel D. More PI is required to restore the intensity of the cutting at **1**:5,6 and **4**:5–8, as seen in panel D, which shows the effect of equimolar PI and porphyrins (2 mol:2 mol per junction). Four-fold excess of PI (panel E) converts both sets of profiles to ones resembling those in the presence of PI alone (panel F). This experiment shows that PI competes for binding sites with both porphyrins, with the ZnTMpyP-4 being more effective than the Ni derivative (see Figure 7C). The dramatic hyperreactivity at **1**:10,11 (Figure 7B-Ni) in the Ni case is not due to tighter binding of NiTMpyP-4. Instead, it must be due to a conformational change in the adjoining DNA which favors $(OP)_2Cu(I)$ reaction or to enhancement of $(OP)_2Cu(I)$ binding in proximity to bound NiTMpyP-4. A curious effect at **4**:12 can be seen in the ZnTMpyP-4 experiment in Figure 7. This position becomes transiently *more* reactive as PI is added (panels C and D), before it attains its final state of low reactivity in the presence of excess PI (panels E and F).

## Discussion

These data provide strong evidence that the region in J1 near the branch point provides a high-affinity binding site for the extended porphyrin ring system as it does for more traditional intercalators (Guo et al., 1989, 1990). These results are of interest in connection with the nature of porphyrin–DNA interactions as well as the special properties of branched DNA which make it a target for intercalative binding agents. Each of the porphyrin derivatives we have tested interacts differentially with the junction in the vicinity of the branch point, as is summarized by the diagram in Figure 8. In each case, differential effects with respect to linear duplexes are detected in a belt of sites surrounding the branch point. The enhancements in $(OP)_2Cu(I)$ scission that we observe here with NiTMpyP-4 and CuTMpyP-4 in particular are much larger than we have seen for any other agents (Figure 8). However, the competition experiment with PI (Figure 7) shows that the mechanism of this hyperreactivity does not involve tighter *binding* by the porphyrins. Rather, some conformation in the adjacent DNA may favor $(OP)_2Cu(I)$ binding and/or scission.

The Ni and Cu porphyrin derivatives have been found capable of intercalation into normal duplex DNA, with a preference for GC sequences, on the basis of several of the stated criteria for intercalation (Pasternack et al., 1983b). The fact that PI competition eliminates the porphyrin enhancement in $(OP)_2Cu(I)$-induced scission is consistent with a model in which these molecules intercalate at or very near the branch point.

The behavior of the axially liganded species is more complicated. The signature of ZnTMpyP-4 interaction with J1 is elimination of the enhancements characteristic of $(OP)_2Cu(I)$-induced cleavage of free J1. Since interaction of ZnTMpyP-4 with J1 is also competitive with PI, are we to conclude that the Zn derivative also intercalates near the branch point of J1? The answer is that we cannot decide from the information available. The effects of the axially liganded porphyrin derivatives on MPE·Fe(II) scission are modest compared to the effects we see on $(OP)_2Cu(I)$ scission. Unfortunately, the mode of interaction of $(OP)_2Cu(I)$ with DNA has not been defined precisely. One hypothesis is that $(OP)_2Cu(I)$ is a partial intercalator itself (Veal & Rill, 1989a,b), so that this process of binding may also be favored by the local structural deformation at the branch point. If the five-coordinate ZnTMpyP-4 also can *partially* intercalate at this site (both MnTMpyP-4 and CoTMpyP-4 are six-coordinate), the strong competition we see for $(OP)_2Cu(I)$ cutting there might reflect the common mode of interaction it shares with the probe. The axially unliganded porphyrins, presumably more fully inserted, may deform the local structure so as to enhance scission by $(OP)_2Cu(I)$ at adjacent positions on the junction arms. However, we should point out that Thederahn et al. (1989) propose a minor groove binding model for the interaction between $(OP)_2Cu(I)$ and duplex DNA, with no obvious insertion of either ring into the helix.

Our investigation of the drug interactions of branched DNAs was stimulated by early observations of Fishel and Warner (1981) that ethidium at very low concentrations could inhibit branch migration in bacteriophage DNA, suggesting some specific interaction at the branch point itself, rather than a more global alteration in the structure of the entire DNA duplexes. This report suggests that porphyrins might exert comparable inhibitory effects, depending strongly on the ionic environment present. Whether the enhancements we observe here are characteristic of other junctions or are specialized for J1 remains to be shown, and one is especially interested in the response of junctions that are not fully sequence immobilized. Finally, it would be of interest to pursue the analogy between enhanced binding of intercalators at DNA branches and at DNA bulges (Williams & Goldberg, 1988), and to establish whether the latter respond to porphyrins in the same way as branches.

ACKNOWLEDGMENTS

We are grateful to Richard Sheardy and Richard Cunningham for helpful discussions.

**Registry No.** $H_2$TMpyP-4, 38673-65-3; CuTMpyP-4, 48242-70-2; NiTMpyP-4, 48242-71-3; ZnTMpyP-4, 40603-58-5; CoTMpyP-4, 51329-41-0; MnTMpyP-4, 72924-08-4.

REFERENCES

Banville, D. L., Marzilli, L. G., Strickland, J. A., & Wilson, W. D. (1986) *Biopolymers 25*, 1837–1858.

Berman, H. M., & Young, P. R. (1981) *Annu. Rev. Biophys. Bioeng. 10*, 87–114.

Bloomfield, V. D., Crothers, D. M., & Tinoco, I., Jr. (1974) *Physical Chemistry of Nucleic Acids*, pp 375–469, Harper and Row, New York.

Bromley, S. D., Ward, B., & Dabrowiak, J. C. (1986) *Nucleic Acids Res. 14*, 9133–9148.

Cantor, C. R., & Schimmel, P. R. (1980) *Biophysical Chemistry*, pp 1239–1264, W. H. Freeman, San Francisco.

Caruthers, M. H. (1982) in *Chemical and Enzymatic Synthesis of Gene Fragments* (Gassen, H. G., & Lang, A., Eds.) pp 71–79, Verlag Chemie, Weinheim.

Carvlin, M. J., & Fiel, R. J. (1983) *Nucleic Acids Res. 11*, 6121–6139.

Carvlin, M. J., Mark, E. H., Fiel, R. J., & Howard, J. C. (1983) *Nucleic Acids Res. 11*, 6141–6154.

Chen, J.-H., Churchill, M. E. A., Tullius, T. D., Kallenbach, N. R., & Seeman, N. C. (1988) *Biochemistry 27*, 6032–6038.

Churchill, M. E. A., Tullius, T. D., Kallenbach, N. R., & Seeman, N. C. (1988) *Proc. Natl. Acad. Sci. U.S.A. 85*, 4653–4656.

Cohen, G., & Eisenberg, H. K. (1969) *Biopolymers 8*, 45–55.

Cooper, J. P., & Hagerman, P. J. (1987) *J. Mol. Biol. 198*, 711–719.

Crothers, D. M. (1971) *Biopolymers 10*, 2147–2160.

Duckett, D. R., Murchie, A. I. H., Diekmann, S., Von Kitzing, E., Kemper, B., & Lilley, D. M. J. (1988) *Cell 55*, 79–89.

Fiel, R. J. (1989) *J. Biomol. Struct. Dyn. 6*, 1259–1275.

Fiel, R. J., Howard, J. C., Mark, E. H., & Datta Gupta, N. (1979) *Nucleic Acids Res. 6*, 3093–3118.

Ford, K. G., Pearl, L. H., & Neidle, S. (1987) *Nucleic Acids Res. 15*, 6553–6563.

Galas, D. J., & Schmitz, A. (1978) *Nucleic Acids Res. 3*, 3157–3170.

Gardner, B. J., & Mason, S. F. (1967) *Biopolymers 5*, 79–86.

Geacintov, N. E., Ibanez, V., Rougee, M., & Bensasson, R. V. (1987) *Biochemistry 26*, 3087–3092.

Gibbs, E. J., Maurer, M. C., Zhang, J. H., Reiff, W. M., Hill, D. T., Malicka-Blaszkiewicz, M., McKinnie, R. E., Liu, H.-Q., & Pasternack, R. F. (1988) *J. Inorg. Biochem. 32*, 39–65.

Gorenstein, D. G. (1984) *Phosphorus 31 NMR*, pp 7–36, Academic Press, New York.

Guo, Q., Seeman, N. C., & Kallenbach, N. R. (1989) *Biochemistry 28*, 2355–2359.

Guo, Q., Lu, M., Seeman, N. C., & Kallenbach, N. R. (1990) *Biochemistry 29*, 570–578.

Hambright, P., Gore, T., & Burton, M. (1976) *Inorg. Chem. 15*, 2314–2315.

Harriman, A., & Porter, G. (1979) *J. Chem. Soc., Faraday Trans. 2 75*, 1532–1542.

Kallenbach, N. R., Ma, R.-I., & Seeman, N. C. (1983) *Nature 305*, 829–831.

Kelly, J. M., Murphy, M. J., McConnell, D. J., & OhGuigin, C. (1985) *Nucleic Acids Res. 13*, 167–184.

Krugh, T. R., & Reinhardt, C. G. (1975) *J. Mol. Biol. 97*, 133–162.

Kuwabara, M., Yoon, C., Goyne, T., Thederhan, T., & Sigman, D. (1986) *Biochemistry 25*, 7401–7408.

Lepecq, J.-B., & Paoletti, C. (1967) *J. Mol. Biol. 27*, 87–106.

Lerman, L. S. (1961) *J. Mol. Biol. 3*, 18–30.

Marky, L. A., Kallenbach, N. R., McDonough, K. A., Seeman, N. C., & Breslauer, K. J. (1987) *Biopolymers 6*, 1621–1634.

Marzilli, L. G., Banville, D. L., Zon, G., & Wilson, W. D. (1986) *J. Am. Chem. Soc. 108*, 4188–4192.

Pasternack, R. F., & Cobb, M. A. (1973) *J. Inorg. Nucl. Chem. 35*, 4327–4339.

Paternack, R. F., Francesconi, L., Raff, D., & Spiro, E. G. (1973) *Inorg. Chem. 12*, 2606–2611.

Pasternack, R. F., Spiro, E. G., & Teach, M. (1974) *J. Inorg. Nucl. Chem. 36*, 599-606.
Pasternack, R. F., Gibbs, E. J., & Villafranca, J. J. (1983a) *Biochemistry 22*, 5409-5417.
Pasternack, R. F., Gibbs, E. J., & Villafranca, J. J. (1983b) *Biochemistry 22*, 2406-2414.
Petrillo, M. L., Newton, C. J., Cunningham, R. P., Ma, R.-I., Kallenbach, N. R., & Seeman, N. C. (1988) *Biopolymers 27*, 1337-1352.
Quigley, G. J., Ughetto, G., van der Marel, G., van Boom, J. H., Wang, A. H.-J., & Rich, A. (1986) *Science 232*, 1255-1258.
Schmitz, A., & Galas, D. J. (1979) *Nucleic Acids Res. 6*, 111-137.
Seeman, N. C. (1982) *J. Theor. Biol. 99*, 237-247.
Seeman, N. C. (1988) *J. Biomol. Struct. Dyn. 5*, 997-1004.
Seeman, N. C., & Kallenbach, N. R. (1983) *Biophys. J. 44*, 201-209.
Seeman, N. C., Maestre, M. F., Ma, R.-I., & Kallenbach, N. R. (1985) in *The Molecular Basis of Cancer* (Rein, R., Ed.) pp 99-108, Alan Liss, New York.
Seeman, N. C., Chen, J.-H., & Kallenbach, N. R. (1989) *Electrophoresis* (in press).
Strickland, J. A., Marzilli, L. G., Gay, K. M., & Wilson, W. D. (1988) *Biochemistry 27*, 8870-8878.
Stryer, L. (1988) *Biochemistry*, 2nd ed., W. H. Freeman, San Francisco.
Thederahn, T. B., Kuwabara, M. D., Larsen, T. A., & Sigman, D. S. (1989) *J. Am. Chem. Soc. 111*, 4941-4946.
Van Dyke, M. W., & Dervan, P. B. (1983a) *Nucleic Acids Res. 11*, 5555-5567.
Van Dyke, M. W., & Dervan, P. B. (1983b) *Cold Spring Harbor Symp. Quant. Biol. 47*, 347-353.
Veal, J. M., & Rill, R. L. (1989a) *Biochemistry 28*, 3243-3250.
Veal, J. M., & Rill, R. L. (1989b) *Biochemistry 28*, 1822-1827.
Wang, J. C. (1974) *J. Mol. Biol. 89*, 783-801.
Ward, B., Skorobogaty, A., & Dabrowiak, J. C. (1986) *Biochemistry 25*, 6875-6883.
Wemmer, D. E., Wand, A. J., Seeman, N. C., & Kallenbach, N. R. (1985) *Biochemistry 24*, 5745-5749.
Williams, L. D., & Goldberg, I. H. (1988) *Biochemistry 27*, 3004-3011.
Young, P. R., & Kallenbach, N. R. (1981) *J. Mol. Biol. 145*, 785-813.

# Cis-Syn Thymine Dimers Are Not Absolute Blocks to Replication by DNA Polymerase I of *Escherichia coli* in Vitro†

John-Stephen Taylor*,‡ and Christine L. O'Day
*Department of Chemistry, Washington University, St. Louis, Missouri 63130*
*Received January 24, 1989; Revised Manuscript Received September 8, 1989*

ABSTRACT: Both *Escherichia coli* DNA polymerase I (pol I) and the large fragment of pol I (Klenow) were found to bypass a site-specific cis-syn thymine dimer, in vitro, under standard conditions. A template was constructed by ligating d(pCGTAT[*c,s*]TATGC), synthesized via a cis-syn thymine dimer phosphoramidite building block, to a 12-mer and 19-mer. The site and integrity of the dimer were verified by use of T4 denV endonuclease V. Extension of a 15-mer on the dimer-containing template by either pol I or Klenow led to dNTP and polymerase concentration dependent formation of termination and bypass products. At ~0.15 unit/$\mu$L and 1-10 $\mu$M in each dNTP, termination one prior to the 3'-T of the dimer predominated. At 100 $\mu$M in each dNTP termination opposite the 3'-T of the dimer predominated and bypass occurred. Bypass at 100 $\mu$M in each dNTP depended on polymerase concentration, reaching a maximum of 20% in 1 h at approximately 0.2 unit/$\mu$L, underscoring the importance of polymerase binding affinity for damaged primer-templates on bypass. Seven percent bypass in 1 h occurred under conditions of 100:10 $\mu$M dATP:dNTP bias, 1% under dTTP bias, and an undetectable amount under either dGTP or dCTP bias. At 100 $\mu$M in each dNTP, the ratio of pdA:pdG:pdC:pdT terminating opposite the 3'-T of the dimer was estimated to be 37:25:10:28. Sequencing of the bypass product produced under these conditions demonstrated that >95% pdA was incorporated opposite both Ts of the dimer and that little or no frame shifting took place. A mechanism whereby products terminating in pdA opposite the 3'-T of the dimer are preferentially elongated by pol I was proposed to account for the higher sequence specificity of the bypass product than the termination product. On the basis of the results of this study, a mechanism was proposed that could account for the origin of the major mutation induced by ultraviolet light in bacteria, the C → T transition mutation at TpdC sites.

The precise mechanisms by which mutagens lead to mutations is not known. One general mechanism is thought to involve error-prone DNA synthesis past DNA damage (lesions) produced by reaction of the mutagen with DNA. The extent and mechanisms by which DNA polymerase are able to synthesize past lesions and the bases that are introduced as a consequence are not well-known or understood [for a review see Strauss (1985)]. One of the best characterized DNA polymerases is pol I[1] of *Escherichia coli* and its large

† This investigation was supported by PHS Grant R01-CA40463, awarded by the National Cancer Institute, DHHS.
* To whom correspondence should be addressed.
‡ Alfred P. Sloan Foundation Fellow.

0006-2960/90/0429-1624$02.50/0 